

NUMERICAL INVESTIGATION OF AERODYNAMICAL PERFORMANCE OF DAMAGED LOW-REYNOLDS AIRFOILS FOR UAV APPLICATION

Ali Doosttalab, Mohammad Mohammadi

Undergraduate Mechanical Engineering Students, K.N.Toosi University of Technology, Iran

Mehdi Doosttalab

R&D Engineer, Nordex Energy GmbH, Germany

Ali Ashrafizadeh

Mechanical Engineering Associate Professor, K.N.Toosi University of Technology, Iran

ABSTRACT

This paper presents two-dimensional numerical investigations and comparison of aerodynamical characteristics at low Reynolds number flow between undamaged and a diversity of differently damaged low-Reynolds and high-lift UAV airfoils. Damages are in form of bullet impact holes in different areas along the chord line (at $0.25c$, $0.5c$ and $0.75c$) and at three different bullet incident angles ($+30^\circ$, 0° and -30°) at mid-chord. Extensive numerical simulations have been done, utilizing the RANS model through solving the Navier-Stokes equations at low Reynolds number of 2×10^5 . The SST-transitional model has been used in the prediction and comparison of the unique flow phenomena prior and after the damages occurrence. The obtained numerical results for undamaged airfoils were compared with the data based on experiments, within less than 5% of error. Numerical simulation processes were performed, using commercial CFD environment, in order to obtain the aerodynamic performances of the proposed model. The results show the significant decrease in aerodynamic performance of the airfoil due to damages done by bullet impact and this degradation in performance is dependent to the damage chord position and impact angle. The CFD calculation results showed that lift coefficient loss increases as the damage location along the chord line moves toward the leading edge especially at higher angles-of-attack. The numerical simulations also showed that increasing the damage angle counter-clock wisely leads to more loss of aerodynamical performances of the airfoil.

INTRODUCTION

One of the vulnerabilities and major concerns in the face of military flying vehicles based on airfoils is the threat of damages to the airfoil structure, caused by impacts with objects such as firearms, ranging from small bullets to large anti-aircraft missiles. In case of unmanned aerial vehicles (UAVs) that fly in low altitudes biggest concern is damages caused by conventional handguns, as a result, UAV survivability is becoming one of the most critical design requirements. In UAV design stage, survivability improvement of the aircraft is exerted, which include prediction of the capabilities of aircraft to survive levels of battle damages. To enhance the survivability of aircraft after damage, a better understanding of aerodynamic behavior of aircraft is required. As a part of this process, vulnerability predictions has tended to concentrate mainly on structural integrity, while only a limited number of studies on the aerodynamics of damaged airfoils have been performed. The aerodynamic stability is the most important for the

continuous operation of an aircraft. When the airfoil is damaged, it effectively generates a flow stream through the hole between high and low pressure areas so it effectively alters aerodynamic characteristics. Airfoils for UAV aircrafts typically operate in Reynolds number range 2×10^5 to 5×10^5 [1]. For example U.S Navy electronic warfare UAVs [2, 3, 4] fly at ship-like speeds ranging from 35 to 40 kn [1]. Two low-Reynolds high-lift UAV airfoils (S1223 and FX 63-137) were chosen for present work [1], at Reynolds number of 2×10^5 .

The accelerated development of CFD (Computational Fluid Dynamics) technology brings us a great opportunity and convenience to perform such works. RANS (Reynolds-Averaged Navier-Stokes) method is generally considered as a possible way in resolve aerodynamic problems [5]. Traditional RANS turbulence models usually assume that the flow is entirely in a turbulent state. However, the laminar to turbulent transition occurs on the surface of the airfoil. That is to say considering the transition can enhance the accuracy of numerical simulations under certain circumstances [6]. A four-equation SST-transitional model is applied in this article to simulate the transition flow over airfoils [7].

NUMERICAL MODELING

Numerical Methods And Turbulence Models

To simulate the flow field, a commercial finite volume CFD code flow solver, which is based upon Reynolds-averaged Navier-Stokes (RANS) equations, was used as a flow solver. The turbulence model which was used in this paper is the four equation SST-Transitional RANS model. The discretion scheme for all equations was the second-order upwind scheme.

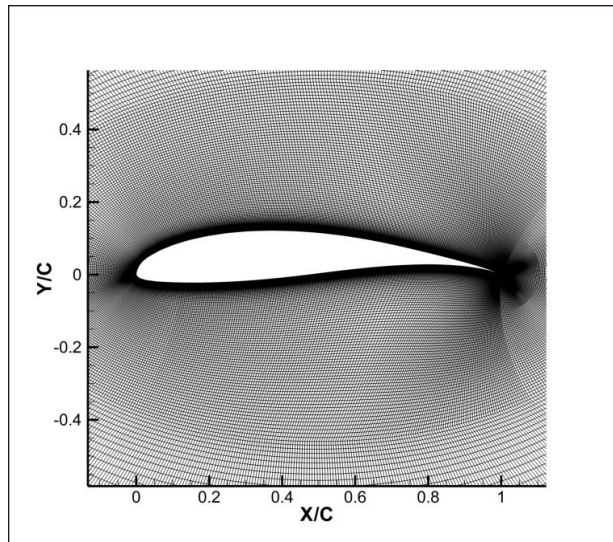


Figure 1. Grid distribution around the airfoil.

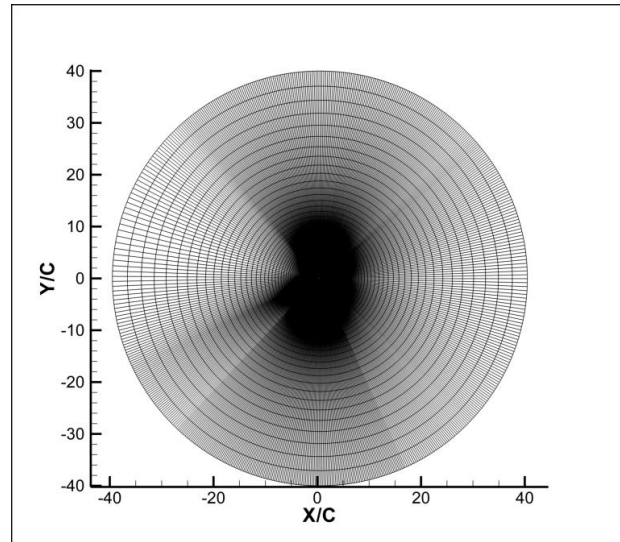


Figure 2. O-type grid.

The GAMBIT grid generator was used to create highly accurate structured mesh around the airfoils. In this investigation O-type mesh was used and the domain of the mesh had a radius of 40 chord lengths in all directions to avoid boundary reflections. The length of numerical airfoil is 1m. Grid contains about 100,000 cells with around 400 grid points on airfoil surface for undamaged airfoils. The height of the first row of cells around the airfoil is set to around $0.00015c$ to maintain the $Y^+ \leq 1$ which is best for utilized SST-Transitional model so that the boundary layer flow can be appropriately resolved.

Damage Modeling

Practically there are a large number of variables involved in the damage range that can affect an airfoil performance. However, for the purpose of studying of a simulated damage, it is more practical to reduce the number of damage forms to a smaller representative number of damages.

As the study of different shapes of damaged has not shown noticeable differences [8]. In the present study, it was considered that the damage is in a form of a two dimensional holes perpendicular to the chord line through a two dimensional airfoil section. Damage size can be expressed in terms of a percentage width of hole formed by the damage to the chord length. The damage size was defined at 0.02% of chord line which is calculated from a damage formed by a conventional 8mm caliber hand gun on a typical UAV airfoil with a 0.4m chord length. Moreover, it was considered a diversity of three different locations of the damages along the chord line at the 0.25, 0.5 and 0.75 of the chord line as shown in Figure 3.

Furthermore as the damage forms may involve different bullet incident angles other than being perpendicular to the chord line, consequently the aerodynamic effects of angle of bullet collide was investigated at the mid chord location with -30 and +30 degrees as shown in Figure 4 and

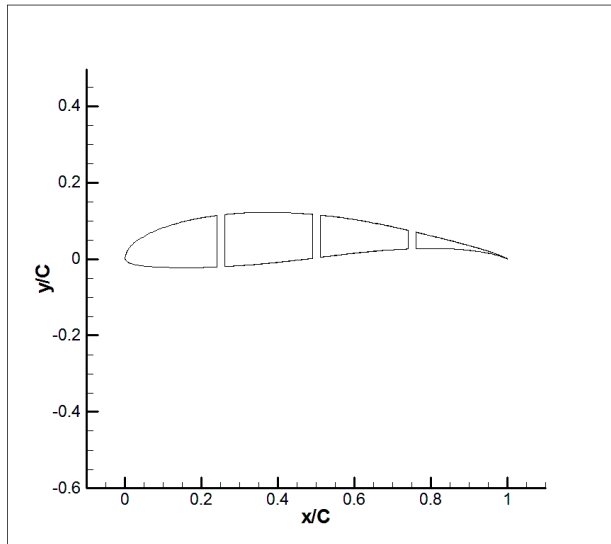


Figure 3. FX63-137 airfoil with holes at 0.25c, 0.5c and 0.75c.

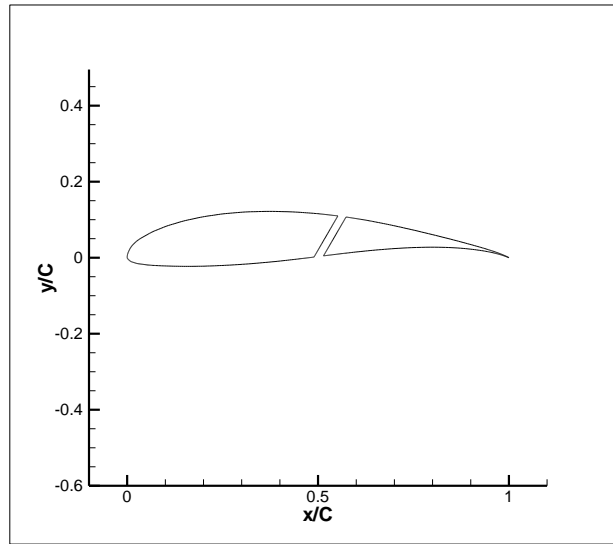


Figure 4. -30 degree bullet incident angle for FX63-137 airfoil.

Figure 5 and the results were compared with the perpendicular hole. The angle of incident of 0 degree is the damage perpendicular to the chord line.

RESULTS AND DISCUSSIONS

Figure 6 and 7 shows respectively for FX63-137 and S1223 airfoils the computed lift coefficients (C_L) of the undamaged airfoils at wide range of angle-of-attack compared with the experimental data, performed in the University of Illinois at Urbana-Champaign (UIUC) open-return subsonic wind tunnel [1]. The numerical results agree well with the experimental data for the angle-of-attack from -5 to stall angle-of-attack well within 5% error and the peak of C_L gained numerically is very close to the measured value.

The effects of damages located at 0.25, 0.5 and 0.75 of chord length at a wide range of angle-of-attack for the FX63-137 and S1223 airfoils are depicted in Figure 6 and Figure 7 respectively. The results at positive angle-of-attack show that loss of C_L increases when the damage location moves towards the leading edge, and the difference become more evident at higher angles-of-attack. It is well known that the S1223 airfoil has better aerodynamical performance than FX63-137 airfoil [1]; however after being damaged the FX63-137 airfoil suffered slightly less C_L loss than the S1223.

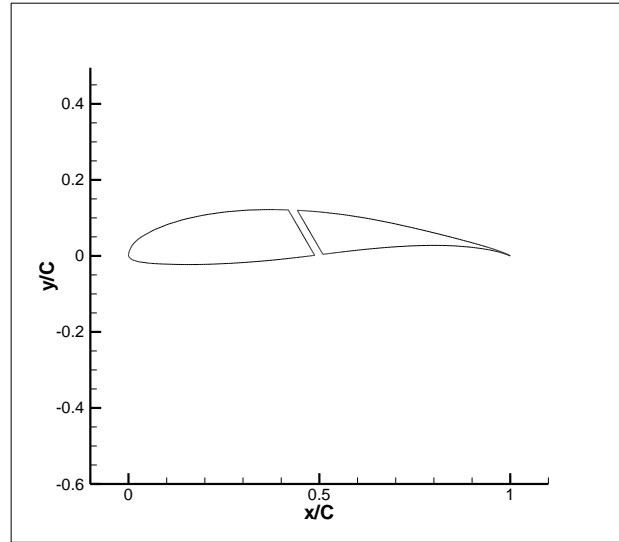


Figure 5. +30 degree bullet incident angle for FX63-137 airfoil.

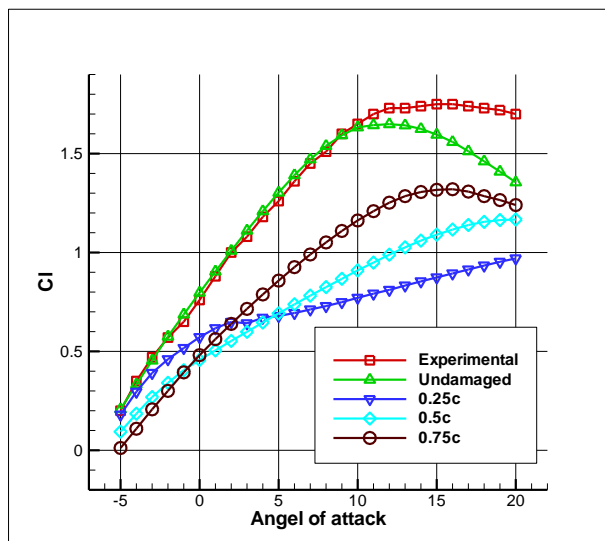


Figure 6. Lift coefficient for FX63-137 airfoil.

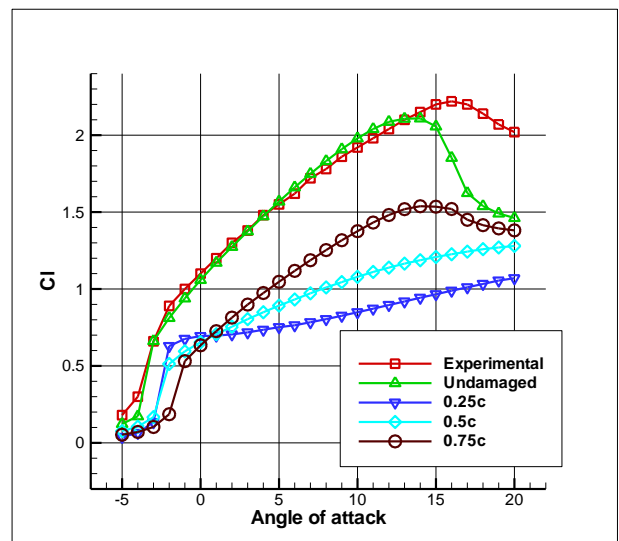


Figure 7. Lift coefficient for S1223 airfoil.

As it can be seen from Figures 6 and 7 as the damage place moves toward the leading edge the stall angle-of-attack increases on the both airfoils.

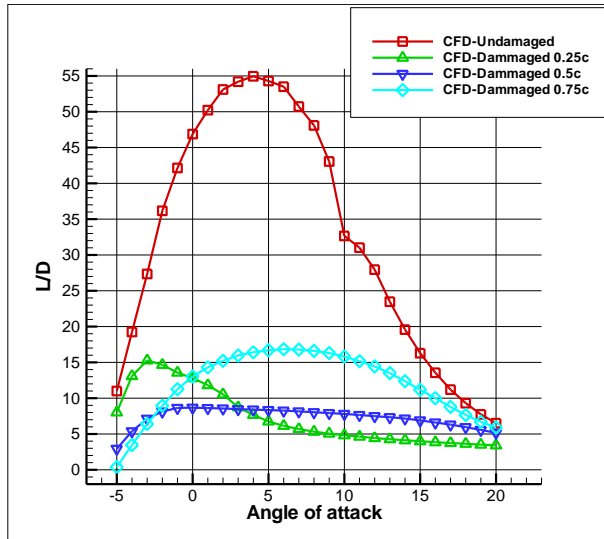


Figure 8. Lift/Drag for FX63-137 airfoil.

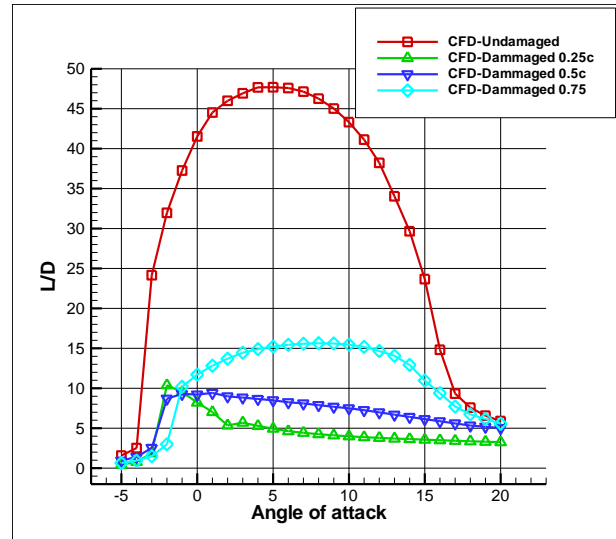


Figure 9. Lift/Drag for S1223 airfoil.

Figure 8 and 9 depicts the effect of differently located damages on Lift/Drag ratio at a wide range of angles-of-attack for the FX63-137 and S1223 airfoils respectively. It is clearly visible that for the both airfoils L/D ratio of damaged airfoils in comparison to undamaged airfoils is highly decreased and in case of damage at 0.25c maximum L/D angle-of-attack is lower but for the damage at 0.75c the maximum L/D angle-of-attack is higher than the undamaged airfoil but the damage also highly flattened the Lift/Drag curve.

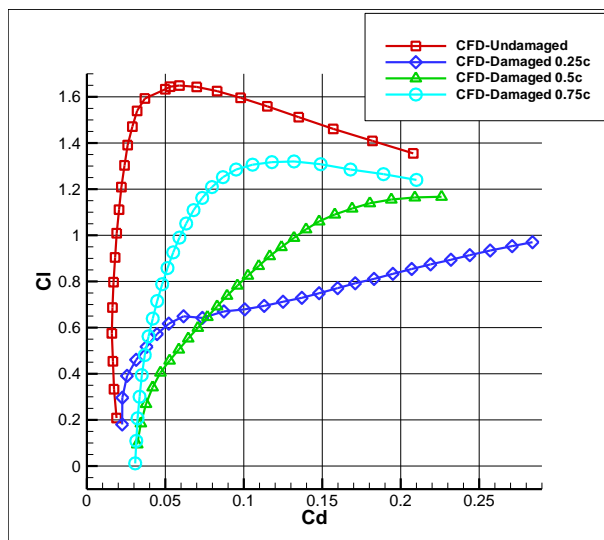


Figure 10. Drag Polar of FX63-137 airfoil.

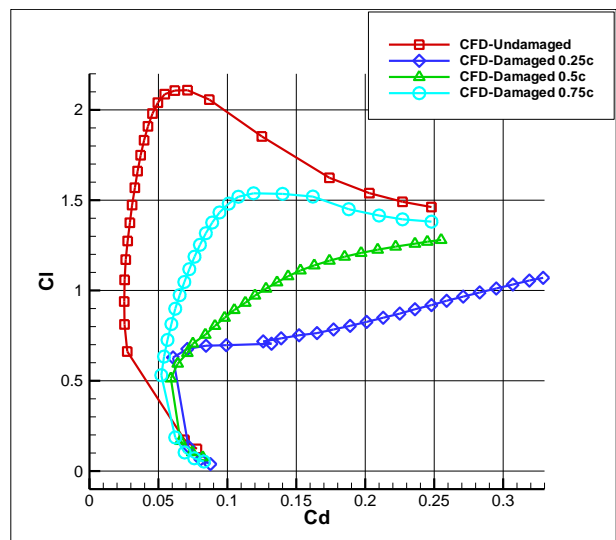


Figure 11. Drag Polar of S1223 airfoil.

The Drag polar of the FX63-137 and S1223 airfoils are presented in Figure 10 and 11. The results show that as the damage moves toward the leading edge the drag increases drastically. For reference, for S1223 airfoil at $C_L=1$ the drag increases 172%, 412% and 1060% for the damages located at 0.75c, 0.5c and 0.25c respectively.

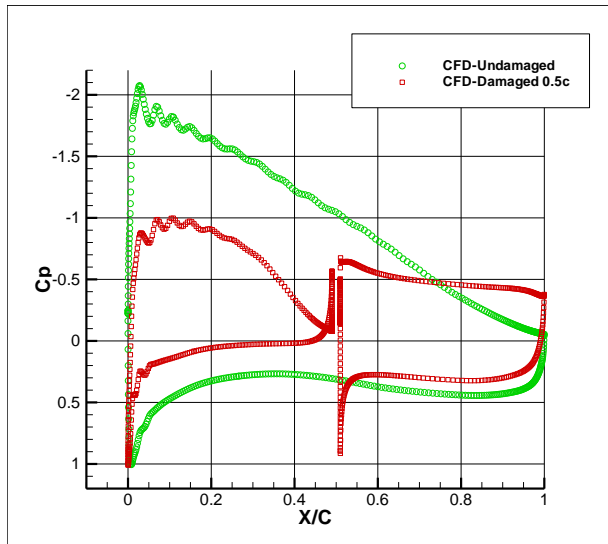


Figure 12. Pressure coefficient for different cord position damages for FX63-137 at angle-of-attack=6 degree.

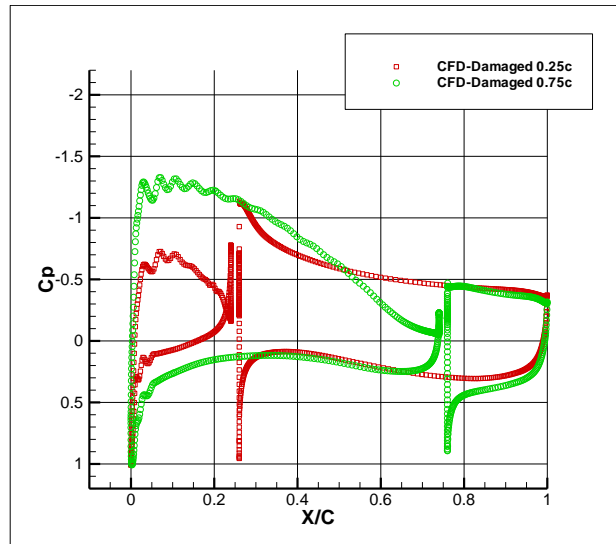


Figure 13. Pressure coefficient for different cord position damages for FX63-137 at angle-of-attack=6 degree.

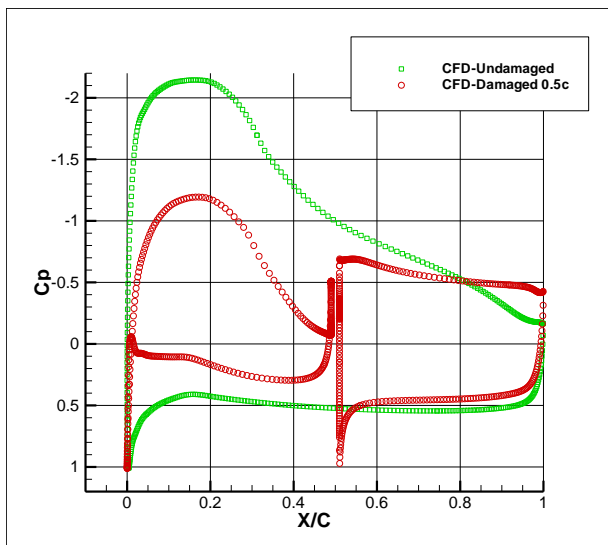


Figure 14. Pressure coefficient for different cord position damages for S1223 at angle-of-attack=6 degree.

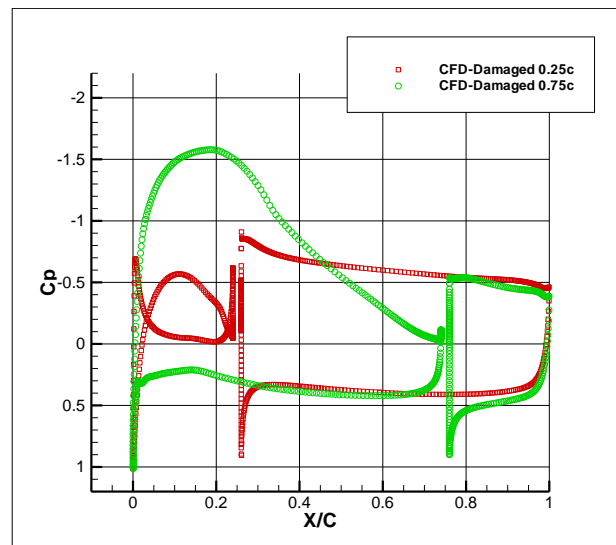


Figure 15. Pressure coefficient for different cord position damages for S1223 at angle-of-attack=6 degree.

The pressure coefficient distributions around damaged and undamaged FX63-137 airfoil are presented in Figure 12 and 13. According to the suction peak chord position which is located nearer the leading edge it can be seen from Figure 13 that the hole nearer the leading edge position decrease the suction peak more intensively thus decreases the C_L , on the contrary at negative angles-of-attack loss of C_L increases when damage position moves toward the trailing edge. At low angles-of-attack (around zero) there is not much difference in C_L between differently located damages and as angle-of-attack increases the difference in C_L of differently located damages become more obvious. The pressure coefficient distributions around damaged and undamaged S1223 airfoil are presented in Figure 14 and 15 and same results observed that the damage nearer the leading edge decrease the suction peak more intensively. As it can be seen from Figure 15, by comparing the pressure coefficient between the damages at $0.25c$ and $0.75c$ it is evident that with the damage at $0.75c$ the upper side of the airfoil has retained the suction peak much better than with the damage at $0.25c$.

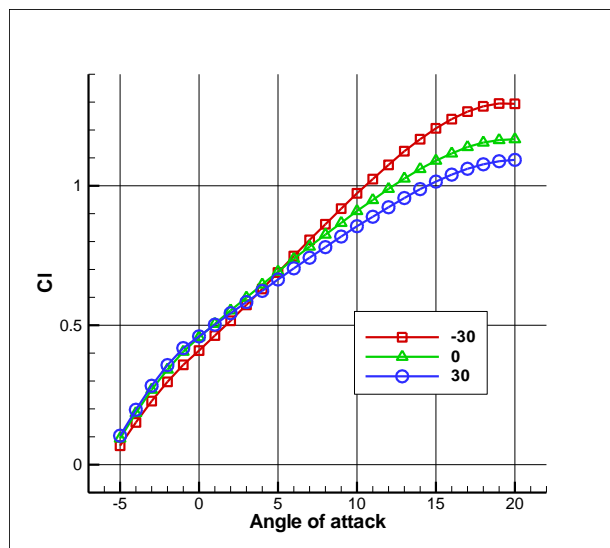


Figure 16. Lift coefficient for different angles of incident for FX63-137 airfoil.

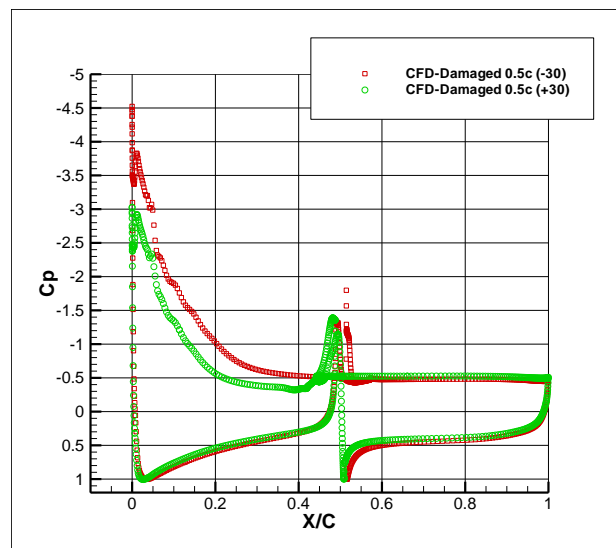


Figure 17. Pressure coefficient for different angle of incident for FX63-137 at angle-of-attack=20 degree.

The effect of the angle of incident of damage is investigated with the Fx63-137 airfoil with damage at 0.5 of chord length with angle of incident of 0 , $+30$ and -30 degrees for the angles-of-attack of -5 to 20 degrees. The angle of incident of 0 degree is the damage perpendicular to the chord line. As shown in Figure 16 damage with angle of incident of $+30$ degree reduced the C_L more severely than the angle of incident of -30 degree at high angle-of-attack, however, there is no significant difference between them at lower angles-of-attack. The reason for better performance of the -30 degree damage angle of incident than the $+30$ angle is that the high pressure air, flows to the upper surface of the airfoil, thus, eliminating the separation bubble from forming. It is also evident from Figure 16 that the angle of incident has no or slight effect on the stall angle-of-attack. The pressure coefficient distribution around the FX63-137 airfoil damaged with $+30$ and -30 degrees angle of incident is presented in Figure 17 at angle-of-attack of 20 degree. The result shows that the airfoil with -30 degree angle of incident has higher suction peak, thus, higher lift coefficient.

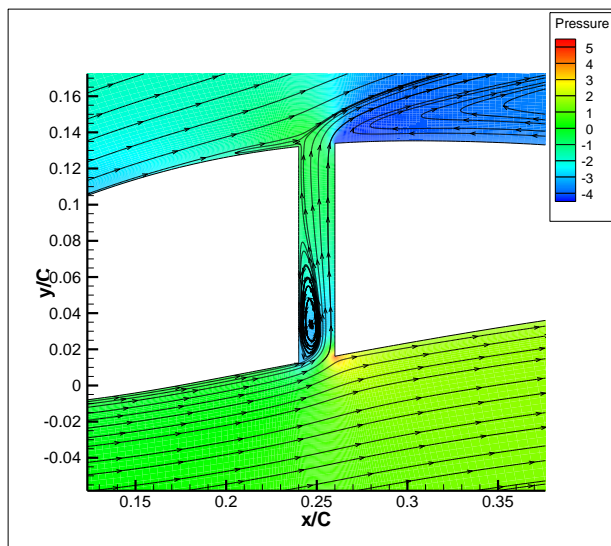


Figure 18. Streamline and pressure coefficient contour around damage on FX63-137 airfoil at 3 degree angle-of-attack.

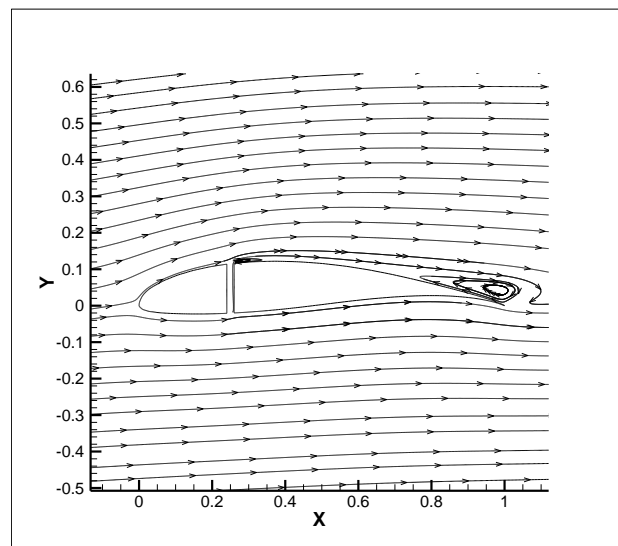


Figure 19. Streamline over damaged FX63-137 airfoil at 3 degree angle-of-attack.

Streamlines and pressure distribution around the damage at 0.25c position hole on FX63-137 airfoil at 3 degree angle-of-attack are depicted in Figure 18. As the streamlines show there is a vortex formed inside of the hole which is a low-pressure region followed by a higher pressure region in the hole above the vortex and also a separation bubble formed downstream of the hole on the upper side of the airfoil.

Figure 19 shows the streamlines over FX63-137 airfoil with damage at 0.25c position at 3 degree angle-of-attack, it can be seen that there is a small separated bubble downstream of the hole which reattached again to the airfoil surface. Furthermore, there is a big separated bubble at trailing edge. With increasing the angle-of-attack, the trailing edge separated bubble moves upstream. At around 5 degree angle-of-attack the trailing edge separated bubble is connected to the smaller separated bubble and creates a big separation bubble downstream of the damage hole.

CONCLUSION

In the present study the aerodynamical characteristics of a diversity of damaged low-Reynolds high-lift UAV airfoils are investigated at Reynolds number of 2×10^5 . The damages are in form of bullet impact holes in different areas along the chord at 0.25c, 0.5c and 0.75c and at three different bullet incident angles of +30, 0 and -30 degrees at mid-chord position. The SST-transitional turbulence model has been used in the prediction and comparison of the unique flow phenomena prior and after the damages occurred. In general, the CFD calculation results showed that lift coefficient loss increases as the damage location along the chord line moves toward the leading edge especially at higher angles-of-attack. The numerical simulations also showed that increasing the damage angle leads to more loss of aerodynamical performances of the airfoil. Also due to highly flattened lift/drag curve and moved maximum lift/drag angle-of-attack, for compensating the lost lift, higher angles-of-attack may be used. Since these investigations are for

a profile of the airfoil thus the actual performance loss of the wings are dependent on the wing span. Furthermore as can be concluded, based on the severity of damage, the UAV maybe controllable, as for the lost lift force we may be able to compensate it by adding lift by ailerons or using higher angles-of-attack, and for the induced drag, thus adverse yaw, in the aircraft we may compensate it by using the rudder, but in any case, the higher drag will increase the energy consumption of the UAV, which affects the nominal range of the vehicle.

CONTACT

Ali Doosttalab

Department of Mechanical Engineering, K.N.Toosi University of Technology, Tehran, Iran

Email: ADoosttalab@asme.org

Mohammad Mohammadi

Department of Mechanical Engineering, K.N.Toosi University of Technology, Tehran, Iran

Email: MohammadMohammadi@asme.org

Mehdi Doosttalab

Nordex Energy GmbH, Langenhorner Chaussee 600 D-22419, Hamburg, Germany

Email: MDoosttalab@nordex-online.com

Ali Ashrafizadeh

Department of Mechanical Engineering, K.N.Toosi University of Technology, Tehran, Iran

Email: ashrafizadeh@kntu.ac.ir

REFERENCES

- [1].Michael S. Selig and James J. Guglielmo, "High-Lift Low Reynolds Number Airfoil Design (Translation Journals style)", Journal of aircraft, vol. 34, No. 1, Jan 1997.
- [2].Foch, J. R., and Toot, P. L., "Flight Testing Navy Low Reynolds Number (LRN) Unmanned Aircraft," Lecture Notes in Engineering: Low Reynolds Number Aerodynamics, edited by T. J. Mueller, Vol. 54, Springer - Verlag, New York, 1989, pp. 407 - 417.
- [3].Foch, J. R., and Ailinger, K. G., "Low Reynolds Number, Long Endurance Aircraft Design," AIAA Paper 92-1263, Feb 1992.
- [4].Bovais, C., and Toot, P., "Flight Testing the Flying Radar Target (FLYRT)," AIAA Paper 94-2144, June 1994.
- [5].Rupesh B. Kotapati-Appara, Kyle D. Squires and James R. Forsythe, "Prediction of the Flow over an Airfoil at Maximum Lift," 42nd AIAA Aerospace Sciences Meeting and Exhibit. Reno, Nevada, January 2004.
- [6].MUELLER T. J., "The Influence of Laminar Separation and Transition on Low Reynolds Number Airfoil Hysteresis (Translation Journalsstyle)", Journal of Aircraft, vol.22, 1985, pp. 764-770.

[7].Selig, M. S., and Guglielmo, J. J., “High-Lift Low Reynolds Number Airfoil Design”, AIAA Paper 94-1866, June 1994.

[8].M.Mani and P.M.Render, Experimental Investigation into the Aerodynamic Characteristics of Airfoils with Triangular and Star Shaped through Damage, 23rd AIAA applied aerodynamic conference, Toronto, Canada, June 6-9, 2005.